

INFLUENCE OF DRIVEN RODS ON PERFORMANCE OF GROUNDING GRIDS IN STRATIFIED SOILS

تأثير إضافة قضبان على خواص شبكات التأسيس لأنواع مختلفة من التربة

M. M. EL-Saadawi

Dept. of Elec. Engineering
Faculty of Engineering
Mansoura University,
Mansoura 35516,
Egypt

I. A. Metwally

Dept. of Elec. Engineering
College of Engineering
Sultan Qaboos University,
P.O. 33, Al-Khod, Muscat-123,
Sultanate of Oman

S. A. EL-Drieny

Dept. of Elec. Engineering
Faculty of Engineering
Mansoura University,
Mansoura 35516,
Egypt

خلاصة

إن التغير في خواص التربة له تأثير كبير على خواص شبكات التأسيس للنظم الكهربائية. وهذا التأثير يمكن قياسه بدلالة مقاومة الأرضى وكل من جهد اللمس وجهد الخطوة. ويؤثر إضافة قضبان إلى شبكات التأسيس على خواصها بدرجة كبيرة.

ويتناول هذا البحث دراسة تفصيلية لتأثير إضافة القضبان على خواص الشبكات الأرضية. وقد تمت دراسة عملية على ثلاثة نماذج لتحاكي أنواع مختلفة من التربة ذات طبقة واحدة أو طبقتين أو ثلاث طبقات مختلفة. ويقدم البحث مقارنة بين النتائج العملية التي تم الحصول عليها مع النتائج النظرية الناتجة من المعادلات الرياضية، وأثبت هذه المقارنة كفاءة استخدام تلك النماذج في دراسة خواص شبكات التأسيس.

Abstract

The variation in soil structure has a great influence on the grounding grid performance. This influence can be measured in terms of ground resistance, touch and step potentials. The addition of driven rods to the grid significantly affects the grounding grid performance. This paper presents a comprehensive experimental study for the influence of adding driven rods on the performance of grounding grids. The study is applied on three constructed scale models. The models have been performed to simulate a single-, double- and triple-layer soils. A comparison between results obtained experimentally and that computed by mathematical equations is introduced.

1. Introduction

Grounding has become one of the dominant problems of system design. As the number and complexity of ac substations increase, the need for accurate design procedures for the grounding system becomes more important both from a safety point of view and for financial considerations. The analytical techniques used have varied from those using simple hand calculations to those involving scale models to sophisticated digital computer programs. The safety of personnel working in a substation has always been of primary concern. With the rising cost of the installation and of grounding systems, a re-evaluation of the design

procedure is in order. The procedure is to design grounding systems for maximum safety against both touch and step potentials. The "touch potential" is that potential, which an individual would experience between feet and hands when touching a "grounded" piece of equipment during a ground fault. "Step potential" is that experienced between an individual's feet spread one meter apart. The grounding system must be so designed that under all fault conditions the maximum tolerable touch and step potential not be exceeded. The analytical techniques used for complex grounding systems are complicated and require some simplifying assumptions to make the digital computer programs manageable [1].

The fault current during an earth fault has several alternate paths for returning to the sources. A part of this current flows between the grounding system and the surrounding earth. The remaining current may return through ground wires or flow through a metallic path consisting of the grounding system conductors and their connection to the neutrals of the supply. The component of the fault current that flows between the grounding system and the surrounding earth is called "grid current". Only this component of the current is responsible for creating dangerous voltages, within or around the station. The grid current may vary from a few percent to almost 100 % of the earth fault current. It depends on the location of the fault, configuration and parameters of ground wires and ground resistance of the station [2].

The fault of high current flows to substation grounding may be the phenomenon of lightning or short-circuit to ground system. It causes potential difference which initiates electrical current paths through human body. If the current is higher than the tolerable for human, the result may vary from shock to death. Good design of substation grounding system is achieved if the grounding system resistance is low with considerable touch and step voltages tolerable for human [3]. A recent study illustrates that a series of serious failures had taken place in China because the ground resistances of some substations did not meet required values [4].

Grounding grid performance is highly dependent on soil structure. In the absence of driven rods, grounding grids with uniform mesh size are quite efficient in soils having a thin, high resistivity top soil [5]. Grids with small mesh size at their peripheries provide optimum performance in uniform soils and soils with low resistivity top soils. Ground rods were found to be effective only when a significant portion of their length is in contact with a low resistivity soil [5]. Most studies presented at this topic are applied to a uniform soil structure [1, 6]. In the work done by Caldecott [1], the water was used to represent the top layer and ager for the bottom layer. The main disadvantage of this model is that the resistivity of the media could not be closely controlled and maintained for a long time. In most previous

studies, the scale models were constructed from galvanized iron, supplied by a 220 V ac through a variac. In this paper the scale models are constructed from aluminum (non-magnetic material) which is suitable for high frequency applications (impulse current test), with 220 V ac power supply. A new suggested method, which provides main features for the influence of driven rods on grounding grids by using scale models (single-layer, double-layer and triple-layer soil for 16-mesh grounding grid with and without 25 driven rods), is experimentally analyzed. A series of experimental configurations for investigation are shown in Fig. 1. The two constructed 16 mesh grids with and without 25 driven rods are consequently shown in Fig.1-a, and Fig.1-b

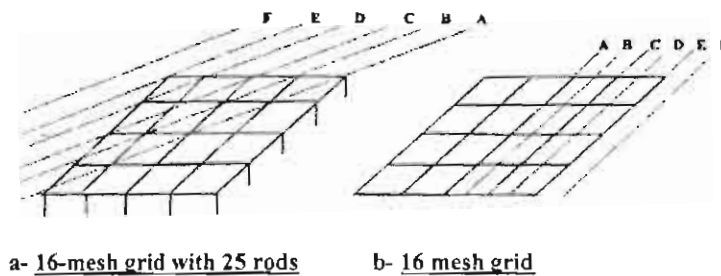


Fig.1 Grid types

2. Simulation of Single-Layer Model

2-1 Model construction

The scale model, of the electrolytic aluminum tank is used for the experiment, has the dimension 0.95 m X 0.95 m X 0.70 m. The model was constructed in the High Voltage Laboratory, Mansoura University, Egypt. Probes consisting of a copper wire were used to measure the surface potential, where only the tip of the wire was touching the surface of the water. The probes were supported on a 'T'-shaped wooden frame, which is rested on the edges of the tank. It could be moved across the surface of the electrolyte at a constant depth in a straight line and in any direction. The grid conductors were made of copper wire with a diameter of 1mm, for a length scale factor of 100:1. Tap water was used as the electrolyte, which serves as an adequately conducting medium and represents homogenous earth. Its electric resistivity, as determined by measuring the total dissolved salts was 21.74 Ω -m. This model was supported below the surface of the electrolyte under tension so as to provide a

horizontal configuration with the minimum distortion. The grid depth is changed by varying the supported height [6].

2-2 Main steps of the experiment

The electrical connection of the measuring system is shown in Fig.2. A 220 V, 50Hz ac supply is used and the tank is grounded. From the applied voltage and current readings, the grid resistance was calculated. The grid was positioned at 2 cm depth. The probe holder was aligned over the centerline of the grid. The potential values are recorded by using voltmeter V_1 at intervals of 2 cm starting from the grid center and ending at approximately 10 cm outside the grid. Due to the symmetry, only one quarter of the grid was investigated [6]. The length of the modeled driven rods was 3 cm. The applied voltage and current were recorded in addition to the surface potential profiles. The potential profiles were recorded along lines parallel to the side of the grid, and along lines parallel to the diagonal of the grid. The profiles are designated by the distance of that profile from the centerline profile or from the diagonal profile. The locations of the profiles were chosen such that maximum and minimum potentials throughout the grid could be determined. Grid resistance is inversely proportional to the scale factor of the model. If a length scale factor of 100 is used, the resistance measured on the model will be 100 times that which would exist in the full-scale situation for the same ground resistivity.

A 16-mesh grid 20 cm X 20 cm, with 25 driven rods of length 3 cm located at each junction of the grid conductors, is used to examine the effect of adding driven rods to the grounding grid.

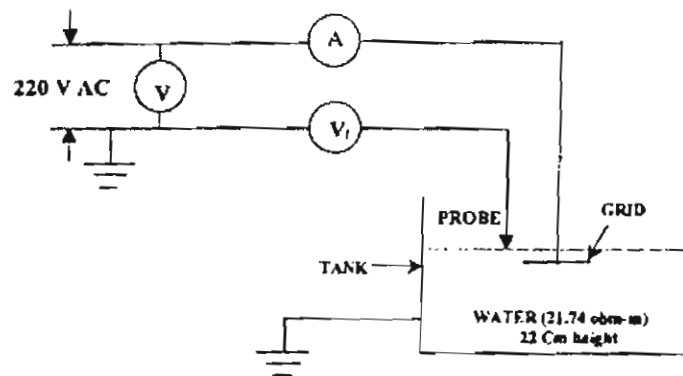
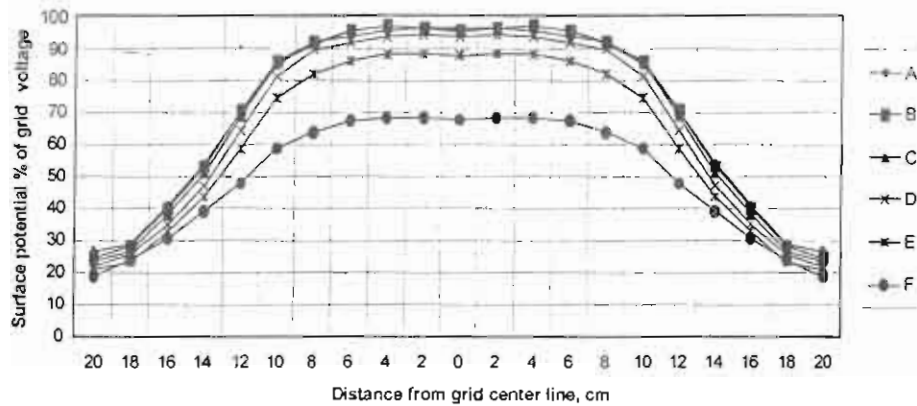


Fig.2 Experimental layout for single layer model

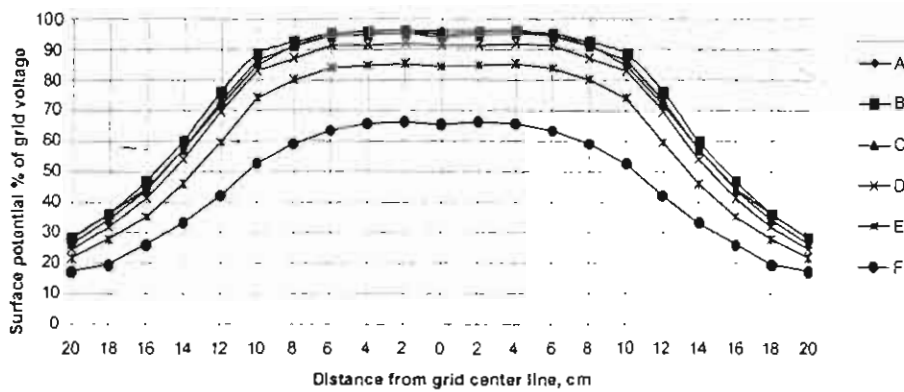
2-3 Experimental results

Typical measured profiles for the 16-mesh grid are shown in Fig.3-a for the normal profiles. Whereas, the results for the normal profiles with 25 driven rods are shown in Fig.3-b. The results for the diagonal profiles are shown in Fig.4-a (without driven rods) and Fig.4-b (with 25 driven rods). The surface potential is given as a percentage of applied grid voltage. From these figures, the maximum and minimum potentials throughout the grid could be determined.

From Fig.3 and Fig.4, it can be concluded that the addition of driven rods decreases the grid resistance (0.3944 Ω before adding the rods and 0.334 Ω after adding 25 rods). The maximum values of touch and step potential also decrease as illustrated by Table 1.

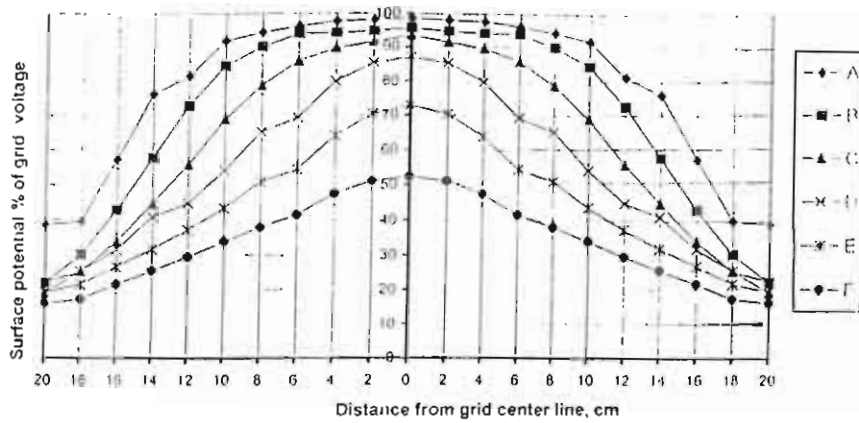


a- without any driven rods

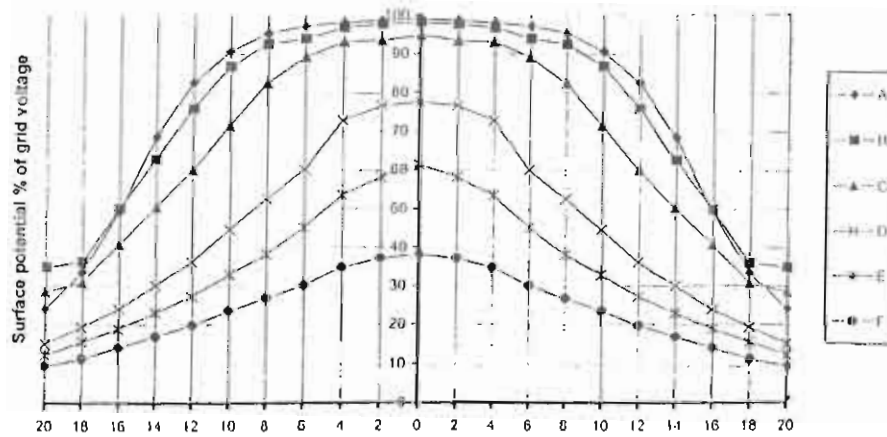


b- with 25 driven rods

Fig. 3 Normal profiles of surface potential for 16-mesh grid in single-layer soil



a- without any driven rod



b- with 25 driven rods

Fig. 4 Diagonal profiles of surface potential for 16-mesh grid in single-layer soil

Table-1 Single-layer percentage touch and step potentials

| Curve no. | Percentage touch potential | | % Reduction in touch potential |
|-----------|----------------------------|---------------------------|--------------------------------|
| | 16 mesh grid | 16 mesh grid with 25 rods | |
| A | 3.9 | 3.5 | 10.26 |
| B | 5 | 4.2 | 16.00 |
| C | 5.9 | 4.66 | 21.02 |
| D | 8.95 | 6.51 | 27.26 |
| E | 15.5 | 11.9 | 23.23 |
| F | 34.5 | 32.1 | 6.96 |

| Curve no. | Percentage step potential | | % Reduction in step potential |
|-----------|---------------------------|---------------------------|-------------------------------|
| | 16 mesh grid | 16 mesh grid with 25 rods | |
| A | 5.17 | 4.17 | 19.34 |
| B | 6.26 | 5.27 | 15.82 |
| C | 6.96 | 5.71 | 17.96 |
| D | 4.66 | 4.56 | 2.14 |
| E | 3.185 | 3.06 | 3.92 |
| F | 2.23 | 1.937 | 12.69 |

2-4 Comparison between experimental and theoretical results

A comparison between experimental and theoretical results of the grid resistance is carried out. The grounding resistance for the grid can be calculated mathematically using

equation A-1 in Appendix A. Whereas, the mesh potential can be computed as a percentage of the grid potential rise by equation B-2 (Appendix B).

The resistance obtained from the scale model is 39.44 Ω (the full scale resistance value is 0.3944 Ω using the scale factor). The comparison results are shown in Table 2. It is noticed that the value of the resistance obtained from the experimental model is close to that obtained mathematically. The deviation percentage is about 1.68 %.

Table 2 Comparison between models and theoretical results

| Grounding grid resistance (Ω) | | | % Mesh (touch) potential | | |
|--|--------------|-----------------------|--------------------------|--------------|----------------------------|
| Scale model | Equation A-1 | %Resistance deviation | Scale model | Equation B-2 | %Touch potential deviation |
| 0.394 | 0.401 | 1.75 | 8.95 | 9.926 | 9.83 |

3. Double-Layer Model

3-1 Model construction

The dimensions of the used constructed aluminum tanks are 0.95 m X 0.95 m X 0.70 m for the bigger tank and 0.91 m X 0.91 m X 0.495 m for the smaller one. Water with different conductivities values is used as the electrolyte, which serves as an adequately conducting medium. The water resistivity can be changed by adding adequate amount of salt. The electric resistivity of each layer is obtained by measuring the total dissolved salts. Arrangement is made to keep the bigger tank on the floor and support the smaller tank on it. The bottom of the upper tank is about 4 cm below the top of the lower tank. The upper tank sides are isolated with a PVC sheet with a height 30 cm from its bottom so that the current passes only through the base of the tank. The resistivities of the water are 21.74 Ω -m and 20 Ω -m for the lower and upper one, respectively. The layout of the system is shown in Fig. 5

3-2 Experimental results

The effective grid resistance can be obtained by measuring the voltage applied to the model and the current flowing through the electrolyte. The potential profiles were recorded by the same way mentioned in the single layer model. The maximum and minimum potentials throughout the grid were determined.

Table 3 illustrates the effect of adding driven rods to the grounding grid. Adding driven rods decrease the grid resistance from 0.3617 Ω to 0.2688 Ω . The maximum values of touch potential decrease between 33.5 to 42.9% and that for step potential decrease between 5.13 to 45.37%.

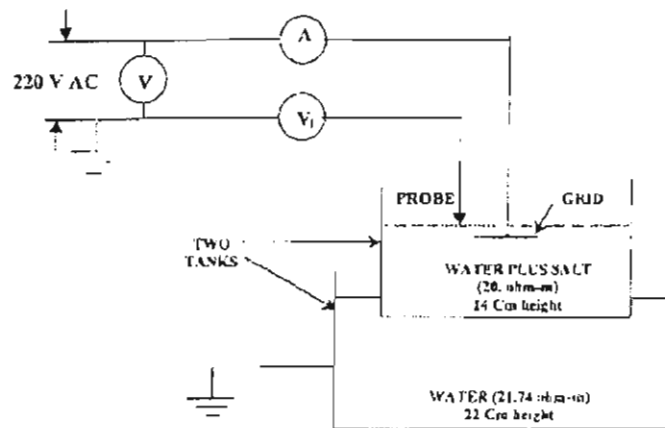


Fig.5 Experimental layout for double-layer model

Table 3 Double-layer percentage touch and step potentials

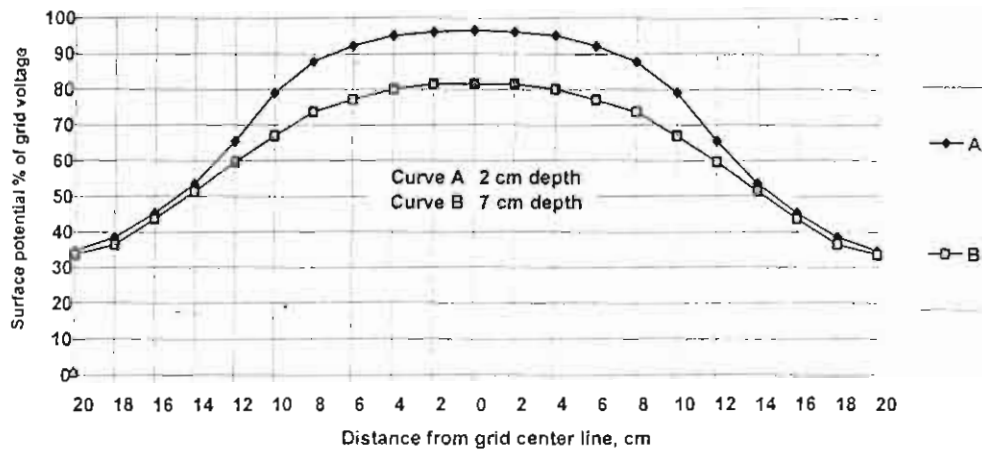
| Curve no. | Percentage touch potential | | % Reduction in touch potential | Curve no. | Percentage step potential | | % Reduction in step potential |
|-----------|----------------------------|----------------------------|--------------------------------|-----------|---------------------------|----------------------------|-------------------------------|
| | 16- mesh grid | 16- mesh grid with 25 rods | | | 16- mesh grid | 16- mesh grid with 25 rods | |
| A | 3.398 | 2.24 | 34.08 | A | 2.92 | 2.77 | 5.13 |
| B | 2.91 | 1.79 | 38.49 | B | 2.69 | 2.48 | 7.80 |
| C | 6.31 | 3.85 | 38.98 | C | 3.46 | 2.195 | 36.56 |
| D | 9.22 | 5.54 | 39.91 | D | 2.27 | 1.24 | 45.37 |
| E | 16.5 | 9.42 | 42.9 | E | 1.77 | 1.16 | 34.47 |
| F | 31.07 | 20.66 | 33.5 | F | 1.82 | 1.23 | 32.41 |

3-3 Comparison between experimental and theoretical results

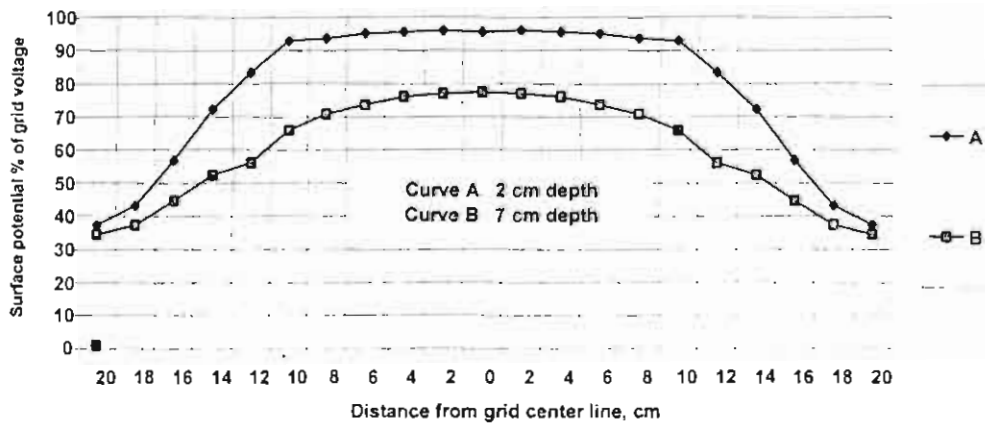
In this case the grounding resistance can be calculated mathematically using equation A-2. Whereas; the mesh potential can be computed as a percentage of the grid potential rise by using equation B-7. The measured resistance is equivalent to 0.3617Ω compared with 0.3766Ω , for the theoretically calculated, with a percentage deviation of 4.13%. The measured touch potential rise has the value of 11.1% whereas; the calculated one is equal to 9.927%.

3-4 Grid depth effect

To examine the grid depth effect on both the step and the touch potentials, the system was tested for two different values of the grid depth, namely 2 cm and 7 cm. Figure 6 represents the normal (Fig. 6-a) and diagonal (Fig. 6-b) profiles of the surface potential for the tested 16-mesh grid. The results show that increasing the grid depth from 2 cm to 7 cm leads to increase in both the percentage touch and step potentials. Table 4 demonstrates the combined effect of grid depth and adding driven rods on both the touch and the step potentials



a) normal profiles



b) diagonal profiles

Fig. 6 Grid depth effect on surface potential for the double-layer model.

Table 4 Grid depth effect on touch and step potential (double-layer model)

| Grid depth | Percentage touch potential | | % Reduction in touch potential | Grid depth | Percentage step potential | | % Reduction in step potential |
|------------|----------------------------|---------------------------|--------------------------------|------------|---------------------------|---------------------------|-------------------------------|
| | 16-mesh grid | 16-mesh grid with 25 rods | | | 16-mesh grid | 16-mesh grid with 25 rods | |
| 2 cm | 3.398 | 2.24 | 34.08 | 2 cm | 2.92 | 2.77 | 5.13 |
| 7 cm | 18.45 | 17.489 | 5.20 | 7 cm | 3.05 | 2.84 | 6.88 |

4. Triple-Layer Model

4-1 Model construction

In this case the used aluminum tanks dimensions are 0.95 m X 0.95 m X 0.70 m, 0.91 m X 0.91 m X 0.495 m and 0.86 m X 0.86m X 0.50 m. Water with different conductivities is used as the electrolyte. The water resistivity is changed by adding adequate amount of salt. The upper and middle tanks' sides are isolated with a PVC sheet with a height 30 cm from the bottom of the tanks. The resistivity of the lower, middle and top tanks are 21.74 Ω -m, 20 Ω -m and 17.86 Ω -m respectively. The layout of the system is shown in Fig. 7.

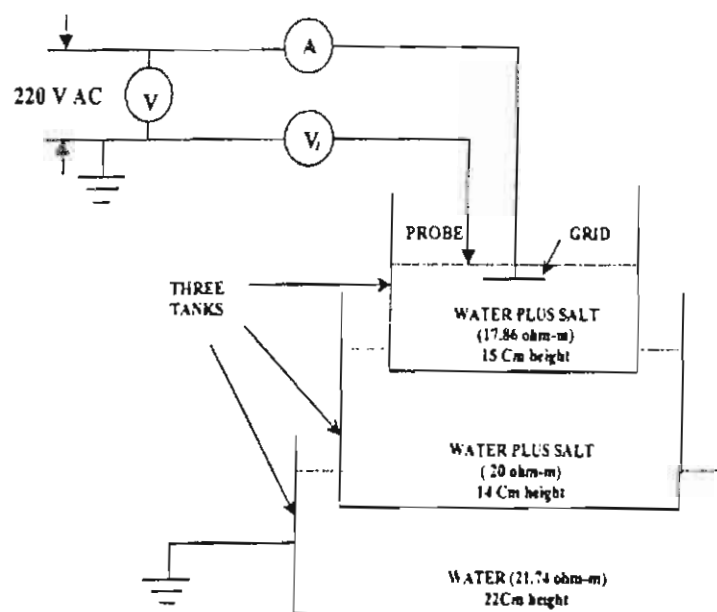


Fig. 7 Experimental layout for triple-layer model

4-2 Experimental results

The main steps of the experiment were repeated for this case. The effective grid resistance, potential profiles, and the maximum and minimum potentials throughout the grid were recorded. The addition of driven rods will decrease the grid resistance (from 0.345 Ω to 0.299 Ω). The results are summarized in Table 5.

Equation A-2 is used to calculate the grounding resistance and equation B-7 to calculate the mesh potential a percentage of the grid potential rise. The measured resistance is equivalent to 0.345 Ω compared with 0.3384 Ω with a percentage deviation of 1.91%. The comparison between measured and calculated results are shown in Table 6

Table 5 Triple-layer percentage touch and step potentials

| Curve no. | Percentage touch potential | | % Reduction in touch potential | Curve no. | Percentage step potential | | % Reduction in step potential |
|-----------|----------------------------|---------------------------|--------------------------------|-----------|---------------------------|---------------------------|-------------------------------|
| | 16-mesh grid | 16 mesh grid with 25 rods | | | 16-mesh grid | 16-mesh grid with 25 rods | |
| A | 2.39 | 1.51 | 36.8 | A | 2.80 | 2.27 | 18.84 |
| B | 2.19 | 1.35 | 38.53 | B | 3.49 | 2.74 | 21.43 |
| C | 6.10 | 3.66 | 40.02 | C | 4.23 | 2.91 | 31.04 |
| D | 8.97 | 5.17 | 42.28 | D | 2.26 | 1.37 | 39.47 |
| E | 14.74 | 8.27 | 43.85 | E | 1.44 | 0.85 | 40.43 |
| F | 28.10 | 18.22 | 35.18 | F | 1.66 | 1.076 | 35.2 |

Table 6 Comparison between experimental and theoretical results (triple-layer model)

| Grounding grid resistance (Ω) | | | % Mesh (touch) potential | | |
|--|--------------|------------------------|--------------------------|--------------|-----------------------------|
| Scale model | Equation A-1 | % Resistance deviation | Scale model | Equation B-2 | % Touch potential deviation |
| 0.345 | 0.3384 | 1.95 | 10.8 | 9.927 | 8.79 |

5. Comparison Between the Three Scale Models

Earth potentials, touch and step voltages are very sensitive to the soil structures in the vicinity of the grounding systems. For low surface soil resistivity the earth surface potentials tend to reach the grid potential leading to low touch and step voltage values (triple-layer model). In this case the current tends to flow laterally away from the grid center rather than downwards. For a higher surface layer resistivity the surface potentials are low because the current tends to flow downwards away from the grid center rather than laterally (single-layer

and double-layer models). The touch and step voltages are expected to be higher in single and double-layer models. The results are demonstrated in Table 7.

Where: - The percentage of touch and step decreasing for triple-layer model are higher than for double-layer model.

- The percentage of touch and step decreasing for double-layer model are higher than for single layer model.

The resistance values are greatly dependent on the location of the grid in the layer. When it is located in a low resistivity layer, the grid resistance is low as shown in Table 8.

Table 7 Percentage touch and step potential decreasing for the three scale models

| % Reduction in touch potential | | | | % Reduction in touch step potential | | | |
|--------------------------------|--------------|--------------|--------------|-------------------------------------|-----------|--------------|--------------|
| Curve no. | Single layer | Double layer | Triple layer | Curve no. | One layer | Double layer | Triple layer |
| A | 10.26 | 34.08 | 36.8 | A | 19.34 | 5.13 | 18.84 |
| B | 16.00 | 38.49 | 38.53 | B | 15.82 | 7.80 | 21.43 |
| C | 21.02 | 38.98 | 40.02 | C | 17.96 | 36.56 | 31.04 |
| D | 28.24 | 39.91 | 42.28 | D | 2.14 | 45.37 | 39.47 |
| E | 23.23 | 42.9 | 43.85 | E | 3.92 | 34.47 | 40.43 |
| F | 6.96 | 33.5 | 35.18 | F | 12.69 | 32.41 | 35.20 |

Table 8 Grounding grid resistance for the three scale models

| Grounding grid resistance (Ω) | | |
|--|--------------|--------------|
| Single-layer | Double-layer | Triple-layer |
| 0.394 | 0.362 | 0.345 |

6. Conclusions

- This paper presents a comprehensive experimental study for the influence of adding driven rods on the performance of grounding grids.
- The addition of driven rods to grounding grid decreases grid resistance, both the maximum value of touch potential and step potential for the three laboratory models.
- The grounding resistance is greatly dependent on the location of grid in the layer.
- Increasing the grid depth leads to the increase in both the touch and step potentials.
- The comparison between the experimental results and the theoretical one was very closed.
- The scale models can be effectively used for studying and verifying the simulation of grounding grid performance.

Acknowledgment

The authors appreciate the facilities made available in the High Voltage Laboratory. Mansoura University. They thank all staff of the laboratory, especially Eng. M. El-Adawy for their helpful assistance.

References

- 1- R. Caldecott and D.G. Kasten, "Scale Model Studies of Station Grounding Grids", IEEE Trans. on power apparatus and systems, Vol. PAS-102, No.3, March 1983, pp.558-566.
- 2- Hans and Arora "A Practical Approach for Computation of Grid Current", IEEE Transaction on power delivery, Vol. 14, No.3, July 1999, pp.897-901.
- 3- B. Phithakwong, N. Krausna, and M. Kando, "New Techniques of the Computer-Aided Design for Substation Grounding", IEEE Power Engineering Society, 2000 Winter Meeting, January 2000, Singapore.
- 4- Q. Meng, J. He, F.P. Dawalibi and J. Ma, "A New Method to Decrease Ground Resistances of Substation Grounding Systems in High Resistivity Regions", IEEE Transaction on power delivery, Vol. 14, No.3, July 1999, pp.911-916.
- 5- H. J. Dawalibi and Jinixi "Efficient Ground Grid Designs in Layered Soils", IEEE Transactions on power delivery, Vol. 13, No.3, July 1998, pp.745-750.
- 6- A. El-Morshedy, A.G. Zeitoun and M.Ghourab, "Modeling of Substation Grounding Grids", IEE proceedings, Vol.133, No.5, July 1986, pp.287-292.
- 7- B. Thapar, and S. I. Goyal, "Scale Model Studies of Grounding Grids in Non-Uniform Soils", IEEE Transactions on power delivery, Vol. PWRD-2, No.4, October 1987, pp.1060-1066.
- 8- M. E. Ghourab, "Modeling of Grounding Grids in Multi-Layer Soils", IEEE Summer Meetings 471-3, 1996.

Appendices

Appendix A: Ground resistance equations in multi-layer soil

A-1 Ground resistance equation in uniform soil

The calculated value of grounding resistance for a grid buried in a uniform soil is given by original paper in [8]:

$$R_g = \rho * [0.25 \sqrt{\pi / A} + (1/L) * [(1 / (2 \pi)) * \ln ((0.165 \times \Delta L) / (2.718 \times D_o))]] * [1 - ((2.256 \times h) / \sqrt{A})] \quad (A-1)$$

where:

- Δl = Mesh side length (m)
- L = Total grid conductor length (m)
- A = Overall area of the grid (m²)
- h = Depth at which the grid is buried (m)
- D_o = Conductor diameter (m)
- ρ = Resistivity of the soil (Ω -m)
- R_g = The grid resistance buried at a depth "h" in uniform soil (Ω)

A-2 Ground resistance equations in double layer soil

In a double-layers soil structure, equation (A-1) is modified due to reflection between the two soils interfaces by original paper in [8]:

$$R_{ig} = R_g - R_p \quad (A-2)$$

Where:

R_{ig} = Resistance of the grid buried at a depth "h" in the upper layer of two-layer soils

$$R_p = \rho_1 \times \ln(1-k) / (2 * 3.14 (h_1+h_0)) \quad (A-3)$$

ρ_1 and ρ_2 = Resistivities of the two layers, Ω -m

$$k = \text{Reflection coefficient and equals to } k = (\rho_2 - \rho_1) / (\rho_2 + \rho_1) \quad (A-4)$$

h_0 and C_p are given by:

$$h_0 = C_t \sqrt{A/2\pi} (\ln(1-k)) * C_p \quad (A-5)$$

$$C_p = (k-1) / 2k \quad (A-6)$$

h_i is the height of the upper layer and C_t is shape factor and is 0.9 for square grids.

Appendix B: Touch and step equations in multi-layer soil

The maximum mesh potential is found at the point within the grid boundary where the surface potential is lowest. The mesh potential is then the potential between this point and the grid; it is in fact the touch potential, E_{touch} that would be experienced by a person standing at this point and touching some apparatus connected to the grid. It is generally found in the corner mesh at a point in its center of the mesh. The maximum percentage value of E_{touch} is given by [6]:

$$E_{touch} = (V_{grid} - V_{min}) / V_{grid} * 100 \quad (B-1)$$

where, V_{min} is the minimum surface potential.

The maximum step potential E_{step} occurs along the diagonal just outside the grid where the slope of the recorded surface potential against distance is maximum. Both mesh and step potentials are normalized to the grid potential so that the results may be compared to the full-scale case [6].

B-1 Touch potential equations in uniform soil

The mesh potential can be calculated mathematically as a percentage of the grid potential rise by original paper in [8]:

$$\% E_{mesh} = 4 r_p k_m k_t * 100 / (1 + 4 r_p) \quad (B-2)$$

where:

r_p = radius of circular plate in meters having the same area as that occupied by the grid.

k_m and k_i = Mesh and current correction factors, respectively; their values are obtained by:

$$K_m = \left[\ln \left(\frac{d_2}{16 \cdot h \cdot d_0} \right) + \frac{(d+2h)^2}{8d \cdot d_0} - \frac{h}{4d_0} \right] + \left(\frac{k_m}{k_h} \right) \cdot \ln \left(\frac{8}{3.14(2n-1)} \right) / (2 \cdot 3.14) \quad (B-3)$$

$$K_i = 0.656 + 0.172 \cdot n \quad (B-4)$$

d = the spacing between parallel conductors,

m and n = number of parallel conductors.

k_{ij} and k_h are calculated by :

$$k_{ij} = 1 / (2n)^{(2/n)} \quad (B-5)$$

$$k_h = (1+h)^{0.5} \quad (B-6)$$

B-2 Touch potential equations in double-layer soil

By taking the non-uniformity correction factor due to different soil resistivities, equation (B-2) is modified to [8]:

$$\% E_{mesh} = 4 r_p C_m k_m k_i \cdot 100 / (1 + 4 r_p) \quad (B-7)$$

where: C_m = the non-uniformity correction factor for mesh voltage and is calculated by:

$$C_m = (\rho_2 / \rho_1)^X \quad (B-8)$$

$$X = \begin{cases} 0.075 \cdot (\log(\sqrt{A} / h_1))^2 & h_1 < \sqrt{A} \\ 0 & h_1 \geq \sqrt{A} \end{cases} \quad (B-9)$$